

Enhancement of the group delay in quadratic coupling optomechanical systems subjected to an external force

Jimmi Hervé Talla Mbé, Ulrich Chancelin Tiofack Demanou, Christian Kenfack-Sadem, and Martin Tchoffo
Citation: Chin. Phys. B, 2023, 32 (**12**): 124202. DOI: 10.1088/1674-1056/accc80
Journal homepage: http://cpb.iphy.ac.cn; http://iopscience.iop.org/cpb

What follows is a list of articles you may be interested in

Ground-state cooling based on a three-cavity optomechanical system in the unresolved-sideband regime

Jing Wang(王婧)
Chin. Phys. B, 2021, 30 (**2**): 024204. DOI: 10.1088/1674-1056/abc159

Cavity optomechanics: Manipulating photons and phonons towards the single-photon strong coupling

Yu-long Liu(刘玉龙), Chong Wang(王冲), Jing Zhang(张靖), Yu-xi Liu(刘玉玺)
Chin. Phys. B, 2018, 27 (**2**): 024204. DOI: 10.1088/1674-1056/27/2/024204

Broadrange tunable slow and fast light in quantum dot photonic crystal structure

Alireza Lotfian, Reza Yadipour, Hamed Baghban
Chin. Phys. B, 2017, 26 (**12**): 124207. DOI: 10.1088/1674-1056/26/12/124207

Time gap for temporal cloak based on spectral hole burning in atomic medium

Abdul Jabar M S, Bakht Amin Bacha, Iftikhar Ahmad
Chin. Phys. B, 2016, 25 (**8**): 084205. DOI: 10.1088/1674-1056/25/8/084205

Entanglements in a coupled cavity-array with one oscillating end-mirror

Wu Qin (吴琴), Xiao Yin (肖银), Zhang Zhi-Ming (张智明)
Chin. Phys. B, 2015, 24 (**10**): 104208. DOI: 10.1088/1674-1056/24/10/104208

Enhancement of the group delay in quadratic coupling optomechanical systems subjected to an external force

Jimmi Hervé Talla Mbé[1,†], Ulrich Chancelin Tiofack Demanou[1,2], Christian Kenfack-Sadem[1], and Martin Tchoffo[1]

[1] *Research Unit of Condensed Matter, Electronics and Signal Processing, Department of Physics, University of Dschang, P.O. Box* 67, *Dschang, Cameroon*

[2] *African Institute for Mathematical Sciences, P.O. Box* 608, *Limbe, Cameroon*

(Received 16 January 2023; revised manuscript received 29 March 2023; accepted manuscript online 13 April 2023)

We theoretically study the effect of the quadratic coupling strength on optomechanical systems subjected to a continuous external force. Quadratic coupling strength originates from strong coupling between the optical and the mechanical degrees of freedom. We show that the quadratic coupling strength reduces the amplitude of the dispersion spectra at the resonance in both blue- and red-sideband regimes. However, it increases (decreases) the amplitude of the absorption spectrum in the blue- (red-)sideband regime. Furthermore, in both sideband regimes, the effective detuning between the pump and the cavity deviates with the quadratic coupling strength. Thereby, appropriate selection of the quadratic coupling strength results in an important magnification (in absolute value) of the group delay for both slow and fast light exiting from the optomechanical cavity.

Keywords: slow and fast light, optomechanical systems, group delay, quadratic coupling

PACS: 42.50.–p, 42.25.Bs, 42.79.–e, 03.65.Yz **DOI:** 10.1088/1674-1056/accc80

1. Introduction

Optomechanical systems have become one of the most attractive topical research subjects in light–matter interactions, from a fundamental viewpoint and in terms of numerous applications (see Ref. [1] for a review) such as entanglement,[2,3] squeezing states,[4–6] normal mode splitting,[7,8] gravitational wave detection,[9] precision measurement, detection, and sensing.[10–14] Recently, their scope of application has widened to include slow and fast light generation through the concept of optomechanically induced transparency (OMIT). Optomechanically induced transparency is a process analogous to electromagnetically induced transparency (EIT)[16–18] and photon-pressure-induced transparency.[19] One of the most significant achievements in the field of slow light was published by Hau *et al.*,[18] where they slowed light to 17 $\mathrm{m{\cdot}s^{-1}}$, using the phenomenon of electromagnetically induced transparency in a condensate of sodium atoms cooled to 50 nK. Since this first experimental observation, research on the subject of slow and fast light has become very diversified. Slow and fast light find practical applications in areas as diverse as interferometry,[20] optical memories,[21,22] all-optical switching and laser radar,[20,23] optical telecommunications,[20] quantum information processing,[24,25] and precision measurements,[26] among others.

Optomechanically induced transparency provides an effective approach to controlling the electromagnetic fields and optical characteristics of matter, and results from the quantum interference of excitation pathways in optomechanical systems. It was successfully used to store light in a cavity and then induce a delay in the output light from the cavity.[27–32] For instance, slow light with a group delay of 0.8 ms was achieved using an optomechanical cavity combined with Bose–Einstein condensate.[31] Furthermore, with single-ended optomechanical cavities, it was also reported that both slow and fast light can be generated if both a coupled and probe laser are considered in an electromagnetically induced transparency configuration.[32] However, these techniques are expensive and difficult to implement.

To realize more controllable optomechanical systems that can simultaneously generate slow and fast light, some authors addressed optomechanical cavities with external force applied to the mobile mirror.[15,16] For instance, Han *et al.* investigated slow and fast light in a hybrid optomechanical system subjected to a time-varying external force.[15] Wu *et al.* studied a simple optomechanical cavity with a constant external force that simultaneously generates slow and fast light.[16] They achieved force-induced light transparency and force-dependent conversion between slow and fast light as a result of the involvement of anti-Stokes and Stokes processes, which were controllable by correctly monitoring the effective pump field power or the external force. However, they did not consider the case of strong coupling between the optical and the mechanical degrees of freedom. Conventionally, the strong coupling regime refers to the case where the optomechanical coupling strength g exceeds the cavity linewidth

†Corresponding author. E-mail: jhtallam@yahoo.fr

© 2023 Chinese Physical Society and IOP Publishing Ltd

κ.[1] Strong coupling can induce the optical cavity mode to be proportional to both the displacement (linear coupling) and the square of the displacement (quadratic coupling) of the mobile mirror in optomechanical systems,[19,34–37] and several experimental implementations to measure and monitor the corresponding coupling strengths have been achieved.[33,38,39] For instance, the quadratic coupling can be tuned by adjusting the tilt of a mobile mirror in a dispersive optomechanical system[38] or measured using homodyne detection in a reflective optomechanical system.[39] Various phenomena have been observed in quadratic optomechanical systems, such as optical cooling and squeezing,[39–42] photon blockade,[43] photon–phonon entanglement,[44] reduction of hysteresis,[45] induction of large transparency efficiency at larger detuning in a hybrid optomechanical system,[46] and only slow light[47,48] or both slow and fast light if a three-level atom is inserted in the cavity.[49] Since the force-induced slow and fast light optomechanical oscillators are easy to control[16] and do not require additional atoms as in Ref. [49], it would be interesting to study the effect of the quadratic coupling in such a system.

In this work, we investigate controllable force-induced slow and fast light optomechanical oscillators which simultaneously experience the linear and quadratic optomechanical couplings. We demonstrate that an appropriate selection of the quadratic coupling parameter enhances (in absolute value) the group delay of both the slow and fast light. The enhancement of the group delay of both the slow and fast light was also addressed using a position-dependent mass optomechanical system, and theoretical variations of the group delay of the order of a few 10 μs were obtained.[50] In the present paper, we show that quadratic optomechanical coupling in an optomechanical cavity subjected to an external force enables the achievement of a more significant variation of the group delay; that is in the order of several hundreds of μs. Besides, the system can be easily controlled by monitoring the external force and the quadratic coupling strength.

The paper is structured as follows. In Section 2, we present the theoretical model and compute the expression of the probe output field and the group delay in both the blue- and red-sideband regimes. In Section 3, we show how the quadratic coupling strength between the optical and the mechanical degrees of freedom contributes to delaying or accelerating the output light. The conclusion is presented in Section 4.

2. Model and calculations

An optomechanical system of the Fabry–Perot type in the presence of an external force acting on the end of the moving mirror and used for the purposes of slow/fast light is presented in Fig. 1. The optomechanical cavity is characterized by a frequency ω_c, a length $L(x=0)$, with x being the displacement of the mobile mirror. The optomechanical cavity is driven simultaneously by a strong pumping field of amplitude ε_p with frequency $\omega_p = 2\pi c/\lambda_p$ and power P_p, and by a weak probe field of amplitude ε_s with frequency $\omega_s = 2\pi c/\lambda_s$ and power P_s. c, λ_p, and λ_s are the velocity of light, and the wavelengths of the pump and the probe fields, respectively. The optical mode characterized by the annihilation operator a (from both the pumping and probe fields) is stored in the cavity at a dissipation rate κ (κ is also known as the cavity linewidth) and interacts via the radiation pressure with the mechanical mode. For simplicity, the mobile mirror is described as a harmonic oscillator in quantum mechanics having a mass m, a frequency ω_m, a damping rate γ_m, and being subjected to an external force f.

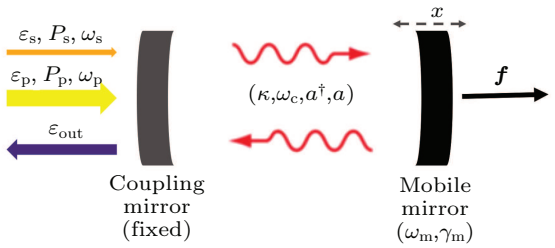


Fig. 1. Schematic diagram of the optomechanical oscillator with an external force. The pump (subscript p) and the probe (subscript s) lights are characterized by $\varepsilon_{p,s}$, $\omega_{p,s}$, and $P_{p,s}$ which stand for their field amplitude, frequency, and power, respectively. x is the displacement of the mobile mirror with frequency ω_m and damping rate γ_m.

When considering strong optomechanical coupling, higher-order terms cannot be neglected in the expansion of the optical resonant frequency in terms of the displacement of the mobile mirror.[37,39–45,47–51] The Hamiltonian of our system yields[16,17,44,45,47–51]

$$H = H_c + H_m + H_{int} - f\cdot x + H_p, \tag{1}$$

with

$$H_c = \hbar\Delta_c a^\dagger a, \tag{2}$$

$$H_m = \left(\frac{p^2}{2m} + \frac{1}{2}m\omega_m^2 x^2\right), \tag{3}$$

$$H_{int} = -\left(\chi x + \frac{\hbar}{2}\mu x^2\right) a^\dagger a, \tag{4}$$

$$H_p = i\hbar\left[\left(\varepsilon_p + \varepsilon_s e^{-i\delta t}\right) a^\dagger - \left(\varepsilon_p + \varepsilon_s^* e^{i\delta t}\right) a\right]. \tag{5}$$

Here H_c describes the free Hamiltonian of the cavity field with $a^\dagger$, the operator creation of the photons in the cavity. H_m represents the Hamiltonian of the mobile mirror with x and p standing for the position and impulse operators, respectively. The term H_{int} represents the Hamiltonian of interaction between the optical modes and the mechanical modes by the effect of radiation pressure with the linear and the quadratic coupling strengths $\chi = \hbar\omega_c/L$ and μ, respectively. The consideration of both coupling strengths expresses the fact that the mechanical and the optical modes of the system are strongly coupled. The Hamiltonian H_p describes the interactions between the cavity

and the two input fields. The pump and the probe field amplitudes are $\varepsilon_{\rm p}=\sqrt{2\kappa P_{\rm p}/\hbar\omega_{\rm p}}$ and $\varepsilon_{\rm s}=\sqrt{2\kappa P_{\rm s}/\hbar\omega_{\rm s}}$, respectively. The term $f\cdot x$ is associated with the external force exerted on the mobile mirror. The force f is constant and can be a magnetic force[51] or a Coulomb force.[52] In these equations, $\delta=\omega_{\rm s}-\omega_{\rm p}$ is the detuning between the pump and the probe and will be called input fields detuning, while $\Delta_{\rm c}=\omega_{\rm c}-\omega_{\rm p}$ is the detuning between the cavity and the pump.

Because we deal with strong optical driving field, quantum fluctuations are ignored and the position, impulse, and cavity field shift to their mean values.[53,54] Using the mean-field approximation $\langle Q\cdot a\rangle\simeq\langle Q\rangle\langle a\rangle$ and transforming the cavity field into a rotating frame at the frequency $\omega_{\rm p}$, the mean value equations of our system are[32,53]

$$\langle\dot{x}\rangle = \frac{\langle p\rangle}{m}, \tag{6}$$

$$\langle\dot{p}\rangle = -m\omega_{\rm m}^2\langle x\rangle+\chi\langle a^\dagger\rangle\langle a\rangle+\mu\langle x\rangle\langle a^\dagger\rangle\langle a\rangle + f-\gamma_{\rm m}\langle p\rangle, \tag{7}$$

$$\langle\dot{a}\rangle = -\left[\kappa+{\rm i}\left(\Delta_{\rm c}-\frac{\chi}{\hbar}\langle x\rangle-\frac{1}{2}\mu\langle x^2\rangle\right)\right]\langle a\rangle + \varepsilon_{\rm p}+\varepsilon_{\rm s}{\rm e}^{-{\rm i}\delta t}. \tag{8}$$

To determine the equilibrium points of the set of Eqs. (6)–(8), the following relationships in terms of the probe field are used:[32,48,49]

$$\langle z\rangle = z_0+z_+\varepsilon_{\rm s}{\rm e}^{-{\rm i}\delta t}+z_-\varepsilon_{\rm s}^*{\rm e}^{{\rm i}\delta t}, \tag{9}$$

where $(z\equiv x,p,a)$. The terms z_0 and $z_\pm$ are the zeroth-order solutions and the first-order perturbation coefficients in the probe field strength $\varepsilon_{\rm s}$, respectively. The three terms in Eq. (9) are in the order associated with the frequencies $\omega_{\rm p},\omega_{\rm s},2\omega_{\rm p}-\omega_{\rm s}$.[16,55] Substituting Eq. (9) into Eqs. (6)–(8) and considering only the lower orders of $\varepsilon_{\rm s}$, the equilibrium points z_0 yield

$$P_0=0, \tag{10}$$

$$a_0=\frac{\varepsilon_{\rm p}}{\kappa+{\rm i}\Delta}, \tag{11}$$

$$x_0=\frac{\chi|a_0|^2+f}{m\omega_{\rm m}^2-\mu|a_0|^2}. \tag{12}$$

The expression of a_+ is also computed as

$$a_+=\frac{\left(\frac{\mu}{m}|a_0|^2+\delta^2-\omega_{\rm m}^2+{\rm i}\gamma_{\rm m}\delta\right)[\kappa-{\rm i}(\Delta+\delta)]-2{\rm i}\omega_{\rm m}\beta}{\left(\frac{\mu}{m}|a_0|^2+\delta^2-\omega_{\rm m}^2+{\rm i}\gamma_{\rm m}\delta\right)\left[\Delta^2+(\kappa-{\rm i}\delta)^2\right]+4\Delta\omega_{\rm m}\beta}, \tag{13}$$

where the parameter

$$\Delta=\Delta_{\rm c}-\frac{\chi}{\hbar}x_0-\frac{1}{2}\mu{x_0}^2 \tag{14}$$

represents the effective detuning between the pump and the cavity and $\beta=\frac{|a_0|^2}{2m\omega_{\rm m}}(\mu x_0+\chi/\hbar)(\mu x_0+\chi)$. Noticeably, Δ is a second-order polynomial of the equilibrium point of the position x_0 obtained by sorting the real root of the following fifth-order polynomial built from Eqs. (11) and (12):

$$\begin{aligned}&\frac{m\omega_{\rm m}^2\mu^2}{4}x_0^5+\left[m\omega_{\rm m}^2\frac{\chi\mu}{\hbar}-f\frac{\mu^2}{2}\right]x_0^4\\&+\left[m\omega_{\rm m}^2\left(\frac{\chi^2}{\hbar^2}-\Delta_{\rm c}\mu\right)-f\frac{\chi\mu}{\hbar}\right]x_0^3\\&-\left[2m\omega_{\rm m}^2\Delta_{\rm c}\frac{\chi}{\hbar}+f\left(\frac{\chi^2}{\hbar^2}-\Delta_{\rm c}\mu\right)\right]x_0^2\\&+\left[m\omega_{\rm m}^2\left(\kappa^2+{\Delta_{\rm c}}^2\right)+2f\Delta_{\rm c}\frac{\chi}{\hbar}-\mu\varepsilon_{\rm p}^2\right]x_0\\&-\left[f\left(\kappa^2+\Delta_{\rm c}^2\right)+\chi\varepsilon_{\rm p}^2\right]=0.\end{aligned} \tag{15}$$

It is important to note that this equation explicitly depends on the pump power through $\varepsilon_{\rm p}$, the external force f, and the quadratic coupling strength μ. The fact that x_0 can be monitored using these parameters brings the advantage of adjusting the effective detuning (see Eq. (14)) by using two external and controllable parameters $P_{\rm p}$ and f, which is necessary to evaluate the field at the exit of the optomechanical cavity.[16] Figure 2 reveals that the equilibrium point of the position x_0 increases with the external force but slightly decreases as the value of the quadratic coupling strength grows. This growth is almost linear with a global slope of about 0.2 nm/mN, meaning that the effective detuning can be controlled directly from the external force (see Eq. (14)). Importantly, it is noted from the inset of Fig. 2 that higher μ allows the variation of x_0 to dwell in larger values. It will then result in an important shift of the detuning from the $\Delta_{\rm c}$ (see Eq. (14)). Table 1 shows the deviations of both the equilibrium point of the position and the effective detuning due to the quadratic coupling strength. Indeed, taking into account the effect of the quadratic coupling strength, there occurs a slight increase (in absolute value) of the equilibrium point of the position x_0 (in the order of fm) from its value when the effect of the quadratic coupling strength is neglected. Yet, such a slight variation of the equilibrium point of the position results in a rise of the effective detuning (see Table 1). Thus, it is necessary to evaluate its effect on the output field.

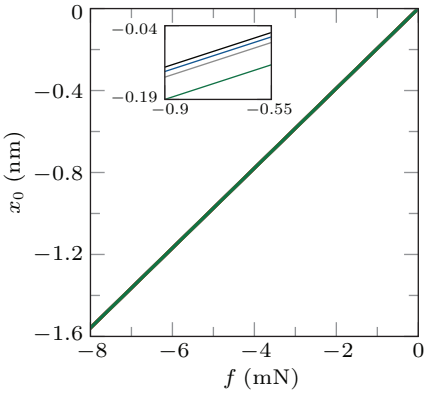


Fig. 2. Equilibrium point of the position versus the external force at different values of the quadratic coupling strength. The inset is an enlargement of the plot. In the inset, from top to bottom, $\mu = (0, 0.1, 1, 3) \times 10^{-9}$ Hz/m^2. $P_{\rm p} = 6 \times 10^{-2}$ W.

Table 1. Variation of the equilibrium of the position and the effective detuning in terms of the quadratic coupling strength, in an acceptable experimental range.[38]

f (mN)	μ (10^{-9} Hz/m^2)	$x_0 - x_0(\mu = 0)$ (fm)	$\Delta - \Delta_{\rm c}$ (kHz)
	0	0	65426.57
	0.1	−0.44	65426.60
−4.74	1	−4.24	65426.87
	2	−8.48	65427.17
	3	−12.71	65427.47
	0	0	53555.50
	0.1	−0.35	53555.52
−3.88	1	−3.44	53555.74
	2	−6.88	53555.98
	3	−10.32	53556.23

2.1. Expression and properties of the light output field

Analysis of the output field will help to study the performance of the quadratic coupling optomechanical oscillator subjected to an external force to slow down or speed up light. This requires evaluation of the absorption and dispersion properties of the output field. Indeed, the input-output relationship is computed as follows:[32,56]

$$\varepsilon_{\rm out} = \varepsilon_{\rm in} - 2\kappa \langle a \rangle , \tag{16}$$

where $\langle a \rangle$ is given by Eq. (9) and the input $\varepsilon_{\rm in} = \varepsilon_{\rm p} + \varepsilon_{\rm s} \, {\rm e}^{-{\rm i}\delta t}$. Substituting these expressions into Eq. (16) yields

$$\varepsilon_{\rm out}(t) = \varepsilon_{\rm out0} + \varepsilon_{\rm out+} \varepsilon_{\rm s} \, {\rm e}^{-{\rm i}\delta t} + \varepsilon_{\rm out-} \varepsilon_{\rm s}^{*} \, {\rm e}^{{\rm i}\delta t} \tag{17}$$

with

$$\varepsilon_{\rm out0} = \varepsilon_{\rm p} - 2\kappa a_0, \tag{18}$$

$$\varepsilon_{\rm out+} = 1 - 2\kappa a_+, \tag{19}$$

$$\varepsilon_{\rm out-} = -2\kappa a_-. \tag{20}$$

Remarkably, the expression of the output field (see Eq. (17)) is similar to Eq. (9). Therefore, the first and the second terms of Eq. (17) also correspond to the pump and the probe fields at frequencies $\omega_{\rm p}$ and $\omega_{\rm s}$, respectively. The third term corresponds to the four-wave mixing field at frequency $2\omega_{\rm p} - \omega_{\rm s}$ and is generated through the interactions between two pump photons and a probe photon via the mechanical mode. For mathematical convenience and without loss of generality, the probe response can be computed through the quadrature

$$\varepsilon_T = 1 - \varepsilon_{\rm out+} = 2\kappa a_+, \tag{21}$$

such that the real part ${\rm Re}\,(\varepsilon_T)$ is responsible for the absorption profile of the output field whereas the imaginary part ${\rm Im}\,(\varepsilon_T)$ displays the dispersion profile of the output field.[30,50,56] Using the equilibrium point of Eq. (13), the expression of such an output field yields

$$\varepsilon_T = \frac{2\kappa}{[\kappa + {\rm i}\,(\Delta - \delta)] + \frac{2{\rm i}\omega_{\rm m}\beta}{\left(\frac{\mu}{m}|a_0|^2 + \delta^2 - \omega_{\rm m}^2 + {\rm i}\gamma_{\rm m}\delta\right) - \frac{2{\rm i}\omega_{\rm m}\beta}{[\kappa - {\rm i}(\Delta+\delta)]}}}. \tag{22}$$

Through the effective detuning, it can be seen that ε_T indirectly depends on x_0. Accordingly, the light transparency can be built by correctly adjusting the external force f or the pump power $P_{\rm p}$ and also the quadratic coupling strength μ (see Eq. (15)). For this purpose, it is necessary to operate in the neighborhood of the first-order red-sideband resonance, i.e., $\Delta \simeq \omega_{\rm m}$, or alternatively in the first-order blue-sideband resonance, i.e., $\Delta \simeq -\omega_{\rm m}$, since it facilitates obtaining normal mode splitting as well as the strongest radiation coupling of the system due to the approximation of the resolved-sideband limit ($\omega_{\rm m} \gg \kappa$).[55] It is important to notice that the first-order red-sideband resonance also corresponds to $\delta \simeq \omega_{\rm m}$ while the first-order blue-sideband resonance is equivalent to $\delta \simeq -\omega_{\rm m}$.[57] Under these considerations, the term $\frac{2{\rm i}\omega_{\rm m}\beta}{[\kappa - {\rm i}(\Delta+\delta)]}$ can be neglected in Eq. (22).

Thus, when the optomechanical system works in the red-sideband regime, it corresponds to the case of a rotating-wave approximation (RWA) and the output field spectra are in the anti-Stokes sideband.[57] Using the approximation $\delta^2 - \omega_{\rm m}^2 \simeq 2\omega_{\rm m}(\delta - \omega_{\rm m})$, the expression of the output is reduced to the following:

$$\varepsilon_{T_{\rm red}} \simeq \frac{2\kappa}{[\kappa + {\rm i}\,(\Delta - \delta)] + \frac{\beta}{\frac{\gamma_{\rm m}}{2} - {\rm i}\left(\delta - \omega_{\rm m} + \frac{\mu}{2m\omega_{\rm m}}|a_0|^2\right)}}. \tag{23}$$

On the other hand, when the optomechanical system operates in the blue-sideband regime, it corresponds to the

case of an anti-RWA and the output field spectra are in the Stokes sideband.[57] Now, the approximation yields $\delta^2-\omega_{\rm m}^2\simeq -2\omega_{\rm m}(\delta+\omega_{\rm m})$ and the output field becomes

$$\varepsilon_{T_{\rm blue}}\simeq\frac{2\kappa}{[\kappa+{\rm i}(\Delta-\delta)]+\frac{\beta}{-\frac{\gamma_{\rm m}}{2}+{\rm i}\left(\delta+\omega_{\rm m}-\frac{\mu}{2m\omega_{\rm m}}|a_0|^2\right)}}. \tag{24}$$

Having computed the output probe field, the next section deals with the calculation of the group delay experienced by that output field.

2.2. Evaluation of the group delay

The group delay experienced in the optomechanical cavities results from the rapid variation in the phase $\phi(\omega_{\rm s})$ of the transmission of the probe field and is defined as[32,57]

$$\tau=\left.\frac{\partial\phi(\omega_{\rm s})}{\partial\omega_{\rm s}}\right|_{\varpi}, \tag{25}$$

where ϖ is the value of the probe frequency at the resonance, i.e., when the value of the transmission of the probe field is equal to 1 and $\phi(\omega_{\rm s}=\varpi)=0$. Indeed, the transmission of the probe field represents the ratio between the probe field returned by the coupling system and the probe field sent to the system and is given by[57]

$$T_{\rm s}(\omega_{\rm s})=\frac{(1-2\kappa a_+)\,\varepsilon_{\rm s}}{\varepsilon_{\rm s}}=1-2\kappa a_+, \tag{26}$$

which by identification with Eq. (19) can be seen as

$$T_{\rm s}(\omega_{\rm s})=|T_{\rm s}(\omega_{\rm s})|\,{\rm e}^{{\rm i}\phi(\omega_{\rm s})}=\varepsilon_{\rm out+}. \tag{27}$$

Noticeably, from Eq. (27), $\phi(\omega_{\rm s})=\arg(T_{\rm s}(\omega_{\rm s}))=\arg(\varepsilon_{\rm out+})$. Therefore, with accurate mathematical investigation, it can be shown that the group delay of Eq. (25) yields

$$\tau=\left.\frac{\partial\phi(\omega_{\rm s})}{\partial\omega_{\rm s}}\right|_{\varpi}=\left.{\rm Im}\left(\frac{1}{\varepsilon_{\rm out+}}\frac{\partial\varepsilon_{\rm out+}}{\partial\delta}\right)\right|_{\delta=\pm\omega_{\rm m}}. \tag{28}$$

According to Eqs. (19), (21), (23), (24), and (28), in either the red-sideband regime or the blue-sideband regime, the probe field escaping from the system can experience a group delay defined as

$$\tau_{\rm red}={\rm Im}\left(-\frac{1}{1-\varepsilon_{T_{\rm red}}}\frac{\partial\varepsilon_{T_{\rm red}}}{\partial\delta}\right)\Bigg|_{\delta=\omega_{\rm m}}, \tag{29}$$

or

$$\tau_{\rm blue}={\rm Im}\left(-\frac{1}{1-\varepsilon_{T_{\rm blue}}}\frac{\partial\varepsilon_{T_{\rm blue}}}{\partial\delta}\right)\Bigg|_{\delta=-\omega_{\rm m}}, \tag{30}$$

respectively.

3. Results and discussion

For our simulations, the values of the parameters are chosen to be within the range of the experimentally accessible values:[16,54] $\lambda_{\rm p}=1064$ nm, $L=25$ mm, $\kappa=2\pi\times215$ kHz, $m=145$ ng, $\omega_{\rm m}=2\pi\times947$ kHz, $\gamma_{\rm m}=2\pi\times141$ Hz, and $\Delta_{\rm c}=-10\omega_{\rm m}$. It is important to mention that with these parameters, strong coupling was achieved from a pumping power of around 0.7×10^{-2} W ($g/\kappa\simeq1.2$).[54] In what follows, κ is kept and the pumping powers are made larger to meet the strong coupling condition ($g/\kappa\gg1$) while maintaining the system in its mean-values state.[1,34,54]

3.1. The red-sideband regime ($\Delta\simeq\omega_{\rm m}$)

In this regime, the expressions of the output probe field and the corresponding group delay are given by Eqs. (23) and (29), respectively.

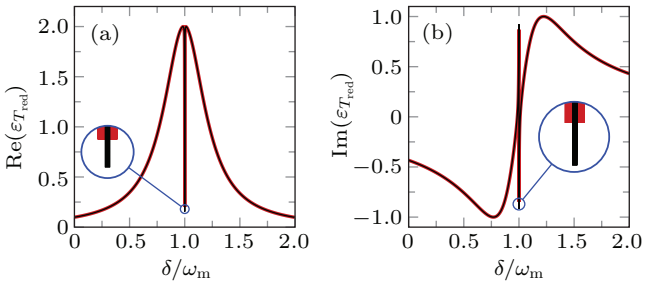


Fig. 3. (a) Real part of the output field. (b) Imaginary part of the output field. For the narrow and the thick lines, the values of the quadratic coupling strength are $\mu=0$ and $\mu=2\times10^{-9}$ Hz/m^2, respectively. For the value of $\delta/\omega_{\rm m}=1$, the narrow line compared to the thick line is always longer at (a) the single end and (b) both ends (see the insets, noting that for (b), to avoid congestion, only one end is enlarged). In the insets, the lengths of the narrow and thick lines are (a) 0.154 and 0.2, respectively; (b) −0.92 and −0.85, respectively. $f=-4.74\times10^{-3}$ N and $P_{\rm p}=6\times10^{-2}$ W.

The plot of the output probe field is sketched in Fig. 3 for $f=-4.74\times10^{-3}$ N. Figures 3(a) and 3(b) represent the real and imaginary parts of the cavity output field as a function of the normalized input fields detuning $\delta/\omega_{\rm m}$, respectively. The real part is called the absorption spectrum (Fig. 3(a)) while the imaginary part is the dispersion spectrum (Fig. 3(b)). As shown in Figs. 3(a) and 3(b), the real and imaginary parts of the probe output field $\varepsilon_{T_{\rm red}}$ vary strongly in the neighborhood of $\delta=\omega_{\rm m}$. From these spectra, let us note that in the presence of the quadratic coupling, the amplitudes at the resonance ($\delta/\omega_{\rm m}=1$) are truncated compared to their values when only the linear coupling is considered (see the insets of Figs. 3(a) and 3(b)). It is important to mention that the results with $\mu=0$ of Fig. 3 are similar to that obtained in Ref. [16] but with an external force of lower magnitude ($f=-4.74\times10^{-6}$ N). The absorption spectrum reveals the appearance of light transparency around the normalized center frequency $\delta=\omega_{\rm m}$ (see Fig. 3(a)). Meanwhile, the dispersion spectrum first grows very rapidly, then suddenly decreases, and finally undergoes an immediate growth with a positive slope (see Fig. 3(b)). This is a prediction of slow light under conditions of OMIT as illustrated in Fig. 4. Indeed, for each value of the quadratic coupling strength, the group delay is positive with a peak occurring exactly at the resonance $\delta=\omega_{\rm m}$; the magnitudes of the

peaks increase as μ increases (Fig. 4). Such an increase originates from the reduction of the negative value of the equilibrium of the position (see Fig. 2) that raises the effective detuning accordingly (see Table 1). For instance, at $\mu = 0$ Hz/m^2, the group delay is equal to $\tau_{\rm red} = 0.380$ ms while it grows to ≈ 0.615 ms when μ reaches 3×10^{-9} Hz/m^2. The difference is estimated to be about 0.235 ms.

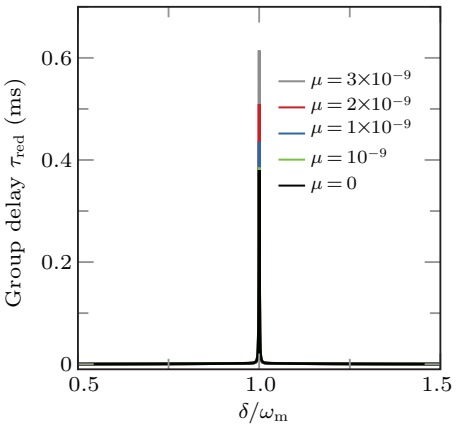


Fig. 4. Group delay of the probe field in the red-sideband regime for different values of the quadratic coupling strength in units of Hz/m^2. $f = -4.74 \times 10^{-3}$ N and $P_{\rm p} = 6 \times 10^{-2}$ W.

3.2. The blue-sideband regime ($\Delta \simeq -\omega_{\rm m}$)

Recall that in the blue-sideband regime the probe output field and the group delay are computed using Eqs. (24) and (30), respectively.

The absorption and the dispersion spectra also depict similar profiles as in the case of the red-sideband regime (see Fig. 5), and with no quadratic coupling it resembles that of the fast light regime of Ref. [16] under weaker force. Nonetheless, it can be seen that the quadratic coupling strength also affects the peak resonances of the absorption and the dispersion profiles as in the case of the red-sideband regime (see Fig. 5). The quadratic coupling strength prolongs the length of the absorption spectrum at the resonance between the input fields detuning δ and the frequency of the mobile mirror $\omega_{\rm m}$ (see the zoomed inset of Fig. 5(a) at $\delta/\omega_{\rm m} = -1$). Contrariwise, under the effect of the quadratic coupling strength, the lengths of the dispersion spectrum at the transparency window are shortened (see the zoomed inset of Fig. 5(b) at $\delta/\omega_{\rm m} = -1$). Compared to the red-sideband regime, the dispersion spectrum shows rather a negative slope with a transparency window around $\delta = -\omega_{\rm m}$, consequently, the group delay is negative (see Fig. 6). This is a signature of the fast light induced by OMIT. With $f = -3.88 \times 10^{-3}$ N, the negative value of the group delay is characterized by a single peak whose magnitude increases (in absolute value) with the quadratic coupling strength μ. We notice that when the quadratic coupling strength is neglected ($\mu = 0$), the group delay is equal to -0.382 ms whereas it changes from about -0.172 ms to reach -0.554 ms when the quadratic coupling strength attains 3×10^{-9} Hz/m^2 (see Fig. 6). As in the red-sideband regime, such an increase is also due to the deviation of the equilibrium of the position of the mobile mirror which results in an augmentation of the effective detuning (see Fig. 2 and Table 1).

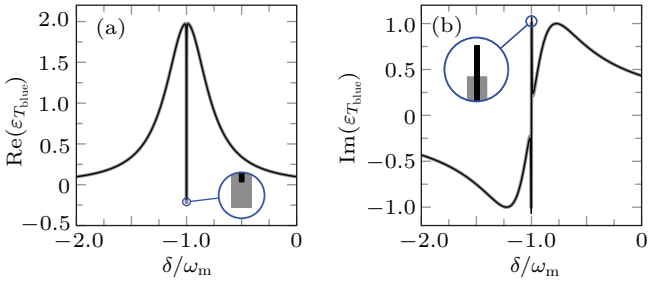


Fig. 5. (a) Real part of the output field. (b) Imaginary part of the output field. For the narrow and the thick lines, the values of the quadratic coupling strength are $\mu = 0$ and $\mu = 2 \times 10^{-9}$ Hz/m^2, respectively. For the value of $\delta/\omega_{\rm m} = -1$, the narrow line compared to the thick line is (a) shorter at the single end, and (b) longer at both ends (see the inset, noting that for (b), to avoid congestion, only one end is enlarged). In the insets, the lengths of the narrow and thick lines are (a) -0.18 and -0.24, respectively; (b) 1.07 and 1.01, respectively. $f = -3.88 \times 10^{-3}$ N and $P_{\rm p} = 6 \times 10^{-2}$ W.

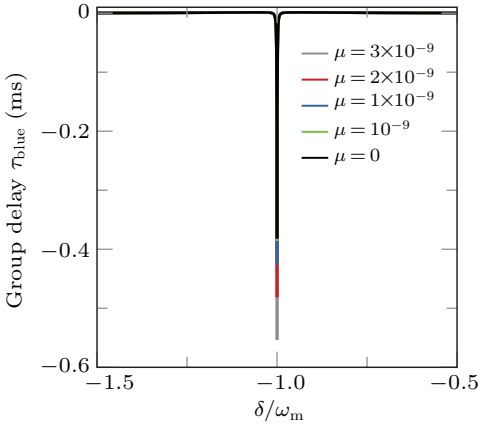


Fig. 6. Group delay of the output field in the blue-sideband regime for different values of the quadratic coupling strength in units of Hz/m^2. $f = -3.88 \times 10^{-3}$ N and $P_{\rm p} = 6 \times 10^{-2}$ W.

3.3. Effect of the input pump power

Another easily tunable parameter of the system is the input pump power $P_{\rm p}$. It is important to analyze its effect on the group delay. Tables 2 and 3 display the results in the red-sideband and blue-sideband regimes, respectively. It appears that in both regimes, whether the quadratic coupling strength is considered or not, the group delay is reduced (in absolute value) when the input pump power is increasing as also observed in hybrid optomechanical systems.[57] The results of Tables 2 and 3 also show a similar decrease (in absolute value) when the quadratic coupling strength is present. However, the fact that the quadratic coupling strength magnifies (in absolute value) the group delay as observed in Subsections 3.1 and 3.2 is also confirmed for different values of the input pump power. Indeed, it can be noticed from Tables 2 and 3 that for a given value of the input pump power $P_{\rm p}$, the group delay is larger (in absolute value) when the quadratic coupling strength is taken into account as compared

to the case where it is neglected. For instance, for a fixed value of the input pump power $P_{\rm p} = 4 \times 10^{-2}$ W and taking two different values of the quadratic coupling strength $\mu = 0$ Hz/m^2 and $\mu = 2 \times 10^{-9}$ Hz/m^2: $-\tau_{\rm red} = 0.577$ ms and $\tau_{\rm red} = 0.78$ ms, respectively (see Table 2); $-\tau_{\rm blue} = -0.578$ ms and $\tau_{\rm blue} = -0.734$ ms, respectively (see Table 3).

Table 2. Variation of the group delay in terms of the input pump power in the red-sideband regime ($\Delta \simeq \omega_{\rm m}$) when the quadratic coupling strength is neglected and when it is considered. $f = -4.74 \times 10^{-3}$ N.

	$P_{\rm p}$ (10^{-2} W)	3	4	5	6
$\mu = 0$ Hz/m^2	$\tau_{\rm red}$ (ms)	0.783	0.577	0.46	0.380
$\mu = 2 \times 10^{-9}$ Hz/m^2	$\tau_{\rm red}$ (ms)	1.1	0.78	0.616	0.51

Table 3. Variation of the group delay in terms of the input pump power in the blue-sideband regime ($\Delta \simeq -\omega_{\rm m}$) when the quadratic coupling strength is neglected and when it is considered. $f = -3.88 \times 10^{-3}$ N.

	$P_{\rm p}$ (10^{-2} W)	3	4	5	6
$\mu = 0$ Hz/m^2	$\tau_{\rm blue}$(ms)	−0.783	−0.578	−0.46	−0.382
$\mu = 2 \times 10^{-9}$ Hz/m^2	$\tau_{\rm blue}$(ms)	−1	−0.734	−0.581	−0.481

4. Conclusion

We have studied the effect of strong optomechanical coupling in the process of slow and fast light generation. Strong optomechanical coupling induces both the linear and the quadratic coupling between the mechanical and the optical degrees of freedom. As demonstrated in Ref. [16], in the absence of external force, the effective detuning is $\Delta \approx \Delta_{\rm c} = -10\omega_{\rm m}$ which is large enough to induce the OMIT expected at the resonance $\Delta = \pm\omega_{\rm m}$. The effect of the external force and the quadratic coupling strength is to bring Δ close to $\pm\omega_{\rm m}$ (Eq. (14)). We have demonstrated that the quadratic coupling strength enhances the effective detuning between the pump field and the cavity. It has been shown that such enhancement affects the light transparency by magnifying the amplitude of the absorption profile of the blue-sideband resonance, and also by shortening the amplitude of the dispersion profile of the blue-sideband resonance and the amplitudes of both the absorption and the dispersion profiles of the red-sideband resonance. Consequently, it increases (in absolute value) the group delay in both the red- and blue-sideband regimes. This prominent result may contribute to the potential applications mentioned above. In future work, we envisage exploring some of these applications.

References

[1] Aspelmeyer M, Kippenberg T J and Marquardt F 2014 *Rev. Mod. Phys.* **86** 1391
[2] Ho M, Oudot E, Bancal J D and Sangouard N 2018 *Phys. Rev. Lett.* **121** 023602
[3] Qin L G, Wang Z Y, Ma H Y, Zhang C M, Ren L, Wang L L and Gong S Q 2019 *J. Opt. Soc. Am. B* **36** 1544
[4] Djorwé P, Nana Engo S G, Talla Mbé J H and Woafo P 2013 *Physica B* **422** 72
[5] Liu L, Hou B P, Zhao X H and Tang B 2019 *Opt. Express* **27** 8361
[6] Huang G, Deng W, Tan H and Cheng G 2019 *Phys. Rev. A* **99** 043819
[7] Hammerer K, Wallquist M, Genes C, Ludwig M, Marquardt F, Treutlein P, Zoller P, Ye J and Kimble H J 2009 *Phys. Rev. Lett.* **103** 063005
[8] Ullah K 2019 *Phys. Lett. A* **383** 3074
[9] Abbott B P 2016 *Phys. Rev. Lett.* **116** 061102
[10] Brawley G A, Vanner M R, Larsen P E, Schmid S, Boisen A and Bowen W P 2016 *Nat. Commun.* **7** 10988
[11] Safavi-Naeini A H, Thourhout D V, Baets R and Van Laer R 2019 *Opt. Express* **6** 203
[12] Brunelli M, Malz D and Nunnenkamp A 2019 *Phys. Rev. Lett.* **123** 093602
[13] Guha B, Mariani S, Lematre A, Combri S, Leo G and Favero I 2018 *Opt. Express* **25** 24639
[14] Xiong H, Liu X Z and Wu Y 2017 *Opt. Lett.* **42** 3630
[15] Han C M, Chen H, Liu W X, Fang A P and Li H R 2019 *Opt. Commun.* **437** 153
[16] Wu Z, Luo R H, Zhang J Q, Wang Y H, Yang W and Feng M 2017 *Phys. Rev. A* **96** 033832
[17] Gu K H, Yan X B, Zhang Y, Fu C B, Liu Y M, Wang X and Wu J H 2015 *Opt. Commun.* **338** 569
[18] Hau L V, Harris S E, Dutton Z and Behroozi C H 1999 *Nature* **397** 594
[19] Bothner D, Rodrigues I C and Steele G A 2021 *Nat. Phys.* **17** 85
[20] Boyd R W and Gauthier D J 2009 *Science* **326** 1074
[21] Xing L, Zhan L, Yi L and Xia Y 2007 *Opt. Express* **15** 10189
[22] Tucker R S, Ku P C and Chang-Hasnain C J 2005 *IEEE J. Lightw. Technol.* **23** 4046
[23] Boyd R W 2009 *J. Mod. Opt.* **56** 18
[24] Chen Y T, Du L, Liu Y M and Zhang Y 2020 *Opt. Express* **28** 7095
[25] Liao Q, Wang X, He G and Zhou L 2021 *Chin. Phys. B* **30** 094205
[26] Yang T Z, Su Y, Xu W and Yang X D 2016 *Appl. Phys. Lett.* **109** 121905
[27] Chen B, Xing H W, Chen J B, *et al.* 2021 *Quantum Inf. Process* **20** 10
[28] Karuza M, Biancofiore M C, Bawaj M, Molinelli C, Galassi M, Natali R, Tombesi P, Di Giuseppe G and Vitali D 2013 *Phys. Rev. A* **88** 013804
[29] Fiore V, Yang Y, Barbour R, Tian L and Wang H 2011 *Phys. Rev. Lett.* **107** 133601
[30] Fiore V, Dong C, Kuzyk M C and Wang H 2013 *Phys. Rev. A* **87** 023812
[31] Chen B, Jiang C and Zhu K D 2011 *Phys. Rev. A* **83** 055803
[32] Tarhan D, Huang S and Müstecaplıoğlu Ö E 2013 *Phys. Rev. A* **87** 013824
[33] Eichenfield M, Chan J, Camacho R M, Vahala K J and Painter O 2009 *Nature* **462** 78
[34] Sommer A de los R, Meyer N and Quidant R 2021 *Nat. Commun.* **12** 1
[35] Mirza I M, Ge W and Jing H 2019 *Opt. Express* **27** 25515
[36] Mirza I M and Van Enk S J 2014 *Phys. Rev. A* **90** 043831
[37] Si L G, Xiong H, Zubairy M S and Wu Y 2017 *Phys. Rev. A* **95** 033803
[38] Sankey J C, Yang C, Zwickl B M, Jayich A M, and Harris J G E 2010 *Nat. Phys.* **6** 707
[39] Vanner M R 2011 *Phys. Rev. X* **1** 021011
[40] Sainadh S and Kumar M A 2015 *Phys. Rev. A* **92** 033824
[41] Purdy T P, Brooks D W C, Botter T, Brahms N, Ma Z Y and Stamper-Kurn D M 2010 *Phys. Rev. Lett.* **105** 133602
[42] Nunnenkamp A, Borkje K, Harris J G E and Girvin S M 2010 *Phys. Rev. A* **82** 021806
[43] Liao J Q and Nori F 2013 *Phys. Rev. A* **88** 023853
[44] Liao J Q and Nori F 2014 *Sci. Rep.* **4** 6302
[45] Djorwé P, Talla Mbé J H, Nana Engo S G and Woafo P 2013 *Eur. Phys. J. D* **67** 1
[46] He Q, Badshah F, Li L, Wang L, Su S L and Liang E 2021 *Ann. Phys.* **533** 2000612
[47] Zhang Y, Yan K, Zhai Z, Bian X, Zuo F, Yu H and Jiang C 2020 *J. Opt. Soc. Am. B* **37** 650
[48] Zhan X G, Si L G, Zheng A S and Yang X 2013 *J. Phys. B: At. Mol. Opt. Phys.* **46** 025501
[49] Wei W Y, Yu Y F and Zhang Z M 2018 *Chin. Phys. B* **27** 034204
[50] Ullah K and Ullah H 2020 *Eur. Phys. J. D* **74** 1
[51] Ma J, You C, Si L G, Xiong H, Li J, Yang X and Wu Y 2015 *Sci. Rep.* **5** 11278
[52] Zhang J Q, Li Y, Feng M and Xu Y 2012 *Phys. Rev. A* **86** 053806
[53] Agarwal G S and Huang S 2010 *Phys. Rev. A* **81** 041803
[54] Gröblacher S, Hammerer K, Vanner M R and Aspelmeyer M 2009 *Nature* **460** 724
[55] Akram M J, Naseer K and Saif F 2015 arXiv:1503.01951 [quant-ph]
[56] Walls D and Milburn G 1994 *Quantum Optics* (Springer-Verlag, Berlin)
[57] Akram M J, Khan M M and Saif F 2015 *Phys. Rev. A* **92** 023846